

# Evaluation of Corrosion Behavior of Al-Mg-Li Alloys in Seawater

Z. Ahmad and Abdul Aleem, B.J.

Weldalite 050, a high-strength Al-Mg-Li alloy, was evaluated for its corrosion resistance in deaerated and air saturated Arabian Gulf water to determine its suitability for marine applications. Weight loss and electrochemical studies showed that the alloy had minimum corrosion rates of 1.82 and 4.82 mpy (mils per year), respectively, in deaerated and air saturated Arabian Gulf water with very high total dissolved solids (TDS) content. Weldalite 050 exhibited good resistance to corrosion at velocities up to 3.9 m/s. The formation of  $\text{Al}_2\text{MgLi}$ , Al-Li,  $\text{Al}_{12}\text{Mg}_{17}$ , and Al-Li precipitates has a pronounced effect on its corrosion resistance. The corrosion resistance of Weldalite 050 compares favorably with that of alloys 5052 and 5054, wrought alloys 6061 and 6013, and silicon carbide (SiC) reinforced alloys 6061 and 6013.

## Keywords

corrosion rate, flow velocity, pitting susceptibility, potentiodynamic polarization, precipitates, ternary phase

## 1. Introduction

UNPRECEDENTED activity in the area of desalination occurred between 1975 and 1985 because of the oil boom in the Arabian Gulf states. Presently, Gulf countries, in particular Saudi Arabia, lead the world in desalinated water production. The Arabian Gulf countries have 27% of the total world desalination capacity, which stands at 3.6 million  $\text{m}^3/\text{day}$  and is expanding further. Cupronickel (90-10) and titanium were the preferred heat exchanger materials. Aluminum alloys of the 5000 series, in particular alloys 5052 and 5054, and alloys 6063 and 6061 from the 6000 series became the focus of attention because of their low initial cost, low maintenance cost in sea coastal environments, and nontoxicity of their corrosion products (Ref 1-4). With the approach of self sufficiency in Gulf countries and the needs dictated by power utility and defense requirements, attention shifted from the conventional to high-strength structural materials capable of resisting long-term environmental degradation. In the latter category, aluminum alloys 2024, 7075, and 6061 and 6013 reinforced with SiC(P) demonstrated high strength and satisfactory resistance to marine corrosion. However, increased fabrication costs, lack of reliable data on the long span environmental degradation, and processing difficulties limited their application.

Simultaneously with the development of fiber-reinforced metal matrix and epoxy composites, the aluminum-lithium alloys underwent a major transformation through a greater scientific understanding of their precipitation behavior and microstructural control of constituent particles, such as  $\text{Al-Cu}_4\text{Fe}$ ,  $\text{Mg}_2\text{Si}$ ,  $\text{FeMnAl}_6$ ,  $\text{CuAl}_2$ ,  $\text{CuMgAl}_2$ ,  $\text{AlCuLi}$ , and  $\text{Al}_2\text{MgLi}$ , which have a profound effect on their strengthening and corrosion characteristics. The family of Al-Li alloys based on Al-Cu-Li (typified by Weldalite 049) and Al-Mg-Li (typified by Weldalite 050) have shown promising application po-

tential as ultrahigh-strength structural materials. Prompted by their highly promising fabrication and mechanical characteristics, the corrosion behavior of Weldalite 050 (Martin-Marietta Corporation, Baltimore, MD) was investigated in Arabian Gulf water. The corrosion performance of this alloy is also compared with the highly promising SiC(P) reinforced Al 6013 and 6061.

## 2. Experimental

### 2.1 Material and Surface Preparation

Samples of Weldalite 050 were used for investigation. Table 1 compares the nominal composition of Weldalite 050 with that of Weldalite 049. Table 2 shows the nominal composition of alloy 6061 and 6013 reinforced with SiC. Specimens in the form of 1.5 cm diam were used.

### 2.2 Test Media

Arabian Gulf water was used for the test. The composition is shown in Table 3.

### 2.3 Surface Treatment

Before the commencement of polarization measurement, the specimens were treated with a hot detergent solution, potable water, ethanol, and 5 V% acetic acid. They were later washed with acetone and demineralized water and dried for 6 h. Specimens after immersion testing were cleaned with a mixture consisting of 50 mL  $\text{H}_3\text{PO}_4$ , 20 g  $\text{Cr}_2\text{O}_3$ , and 85 wt% water at 70 to 80 °C for 3 min.

For metallographic examination, the specimens were ground to 400 and 600 SiC grit finish to remove coarse scratches. Final grinding was done to a 0.3  $\mu$  SiC grit finish. They were then rinsed with acetone, distilled water, and in a

Table 1 Nominal composition of Weldalite

Alloy type	Composition, wt %					
	Mg	Li	Ag	Zr	Cu	Al
050	5.19	2.08	0.39	0.14	0	Balance
049	0.37	1.21	0.19	0.17	6.20	Balance

Z. Ahmad and Abdul Aleem, B.J., King Fahd University of Petroleum & Minerals, Dhahran-31261, Saudi Arabia. Z. Ahmad is presently at Center for Advanced Material, Penn State University, University Park, MD 16801, USA.

**Table 2 Nominal composition of alloys 6061 and 6013 reinforced with SiC**

Alloy	Composition, wt %								Unspecified other element, each	Unspecified other element, total	Minimum Al
	Si	Fe	Cu	Mn	Cr	Zn	Mg	Ti			
6061	0.4-0.8	0.7	0.15-0.4	0.15	0.8-1.2	0.04-0.3			0.05	0.15	Remaining
6013	0.6-1.0	0.5	0.6-1.1	0.2-0.8	0.1	0.25	0.8-1.2	0.1	0.01	0.15	Remaining

**Table 3 Nominal composition of Arabian Gulf water**

Compound	Nominal composition, ppm
Na <sup>+</sup>	15,478
Ca <sup>++</sup>	780
Mg <sup>+</sup>	1,667
SO <sub>4</sub> <sup>2-</sup>	4,134
Cl <sup>-</sup>	28,026
HCO <sub>3</sub> <sup>-</sup>	148
SiO <sub>2</sub>	2.0
TDS	50,272

TDS is total dissolved solids.

steam of air prior to examination by scanning electron microscopy (SEM).

## 2.4 Corrosion Data Analysis

### 2.4.1 Immersion Testing

Corrosion rates were determined by immersion testing in accordance with the recommendation of ASTM designation G-64 (reapproved 1990) (Ref 5). The corrosion rates are reported in mdd (milligrams per decimeter square per day) and mpy (mils per year).

### 2.4.2 Electrochemical Testing

The corrosion rates were determined by potentiodynamic and polarization resistance techniques recommended by ASTM designation G-31-72 (Ref 6). Both the polarization measurements (Tafel plots and polarization resistance) were started from open circuit potential achieved after 45 min of immersion in seawater. A scanning rate of 0.5 mV/s was used. An EG & G model 273 potentiodyne fitted with a microprocessor was used. An EG & G softcorr program was used.

## 3. Results and Discussion

Results of weight loss studies of Weldalite 050 in Arabian Gulf water are given in Table 4.

The corrosion rate decreased with exposure time, and after 1500 h of exposure, it reached a near steady state. Duplicates were used. Similar phenomena were reported for wrought aluminum alloys 6061 and 6013 and alloys reinforced with SiC. The decreased corrosion rate with increased exposure time was attributed to the kinetics of dissolution and growth of a protective film of Al(OH)<sub>3</sub>, whose presence was confirmed by x-ray diffraction (XRD), Fourier transformation infrared spectroscopy (FTIR), and electron dispersive analysis by x-ray (EDX) studies. The presence of a duplex film comprised of an outer

**Table 4 Variation of corrosion rate with exposure time for Weldalite 050**

Exposure time, h	Corrosion rate, mpy
500	3.4
800	3.0
1000	2.5
1500	2.0

**Table 5 Corrosion rate of Weldalite 049**

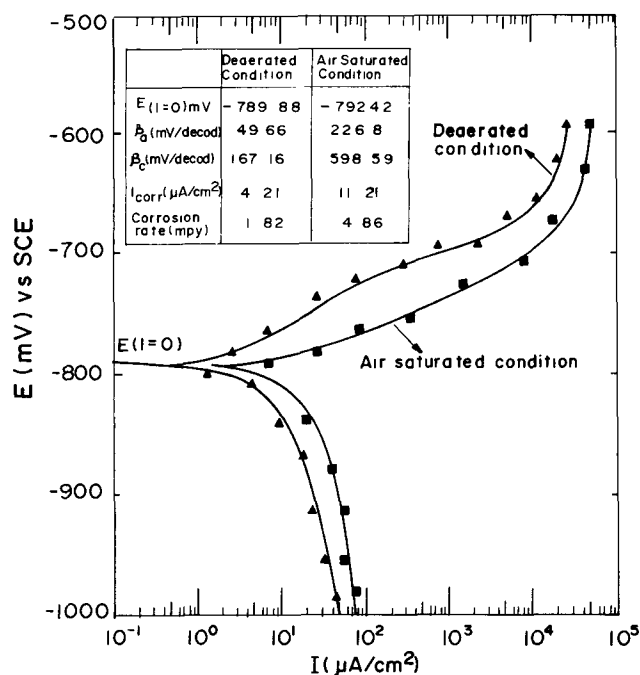
Composition, % Cu	Corrosion rate		Pit depth, μm
	mdd	mpy	
6.3	5.1	2.91	320
5.4	5.2	2.99	180
5.0	4.0	2.80	130

mdd is milligrams per decimeter square per day. mpy is mils per year.

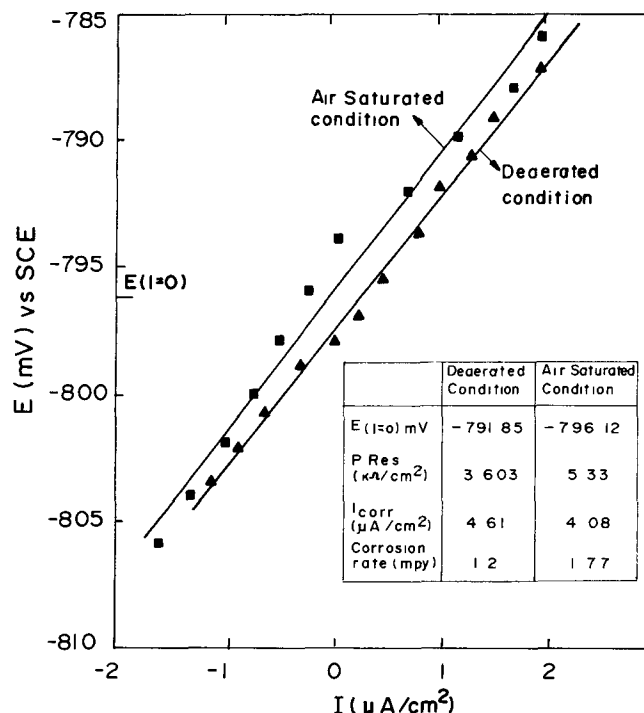
porous layer and an inner compact layer in aluminum alloys 5454 and 6061 was reported (Ref 7). Changes in the outer porous layer because of corrosion affects the dissolution kinetics of the inner layer by allowing a flux of reactants (mostly OH<sup>-</sup>) to reach the inner compact layer. Once the inner compact layer achieves a uniform thickness, the corrosion rate is leveled, as shown by the results in Table 4. Weldalite 050, with no Cu, showed a better corrosion resistance than Weldalite 049, with Cu, as shown in Table 5 (Ref 8).

Table 1 gives the composition of Weldalite 049. Table 5 shows that the pitting depth increased with increased Cu concentration. The lowest corrosion rate was obtained with 5% Cu. Whereas the Cu containing precipitates impart high mechanical strength, they also increase the susceptibility to corrosion and stress-corrosion cracking (SCC) in marine environment (Ref 9). The decreased corrosion resistance of Weldalite 049, which contains Cu, is due to the formation of Al<sub>2</sub>Cu Li precipitates, whose presence was confirmed by transmission electron microscopy (TEM) studies. The corrosion resistance of Weldalite 050 is increased by the absence of the above precipitate.

The results of electrochemical studies on alloy 050 are summarized in Table 6 and illustrated in Fig. 1 and 2. Note that Arabian Gulf water is highly corrosive because of a very high concentration of TDS. TDS concentration may reach as high as 50,000 ppm, which exceeds the average TDS concentration of any other ocean. The difference between the corrosion rate obtained by linear polarization (1.77 mpy) and Tafel extrapolation (4.86 mpy) in air saturated Gulf water is due to a larger



**Fig. 1** Potentiodynamic polarization plot of Weldalite 050 in deaerated and air saturated Arabian Gulf water at 25 °C



**Fig. 2** Representative polarization resistance plot of Weldalite 050 in Arabian Gulf water

**Table 6** Summary of potentiodynamic tests of Weldalite materials in Arabian Gulf water

Weldalite 050	Polarization resistance					Tafel analysis				
	$E(I=0)$ , mV	Polarization resistance, $K \cdot \Omega/cm^2$	$I_{corr}$ , $\mu A/cm^2$	Corrosion rate, mpy	Corrosion rate, mdd	$E(I=0)$ , mV	$\beta_a$ , mV/decade	$\beta_c$ , mV/decade	$I_{corr}$ , $\mu A/cm^2$	Corrosion rate, mpy
Deaerated condition	-791.85	3.60	4.61	1.2	2.22	-789.88	49.66	167.16	4.21	1.82
Air saturated condition	-796.12	5.33	4.08	1.77	3.27	-792.42	226.8	598.59	11.21	4.86

$E(I=0)$  is corrosion potential.  $\beta_a$  is anodic Tafel constant.  $\beta_c$  is cathodic Tafel constant.  $I_{corr}$  is corrosion current density. To convert mils per year (mpy) to mm/year, multiply by  $2.5 \times 10^{-3}$ . To convert mdd to mm/year, multiply by  $0.03652/\rho$ .  $\rho$  is density,  $g/cm^3$ .

**Table 7** Effect of velocity on the corrosion rate of Weldalite 050

Velocity, m/s	Brackish water		Arabian Gulf water	
	mpy	mdd	mpy	mdd
1.3	5.18	9.58	6.08	11.24
1.9	6.20	11.47	6.92	12.80
2.7	7.9	14.63	8.66	16.02
3.8	8.92	16.50	9.32	17.24

Brackish water contains ~2000 ppm total dissolved solids (TDS).

degree of deviation from the corrosion potential in the latter. The corrosion potential ( $E_{corr}$ ) of Weldalite alloy 050 observed in deaerated seawater was lower than that observed in air saturated seawater. The corrosion rate of Weldalite 050 observed in deaerated seawater (1.82 mpy) was lower than that observed in air saturated seawater (4.86 mpy). The electrochemical results closely agree with the weight loss results.

The higher SCC resistance of Weldalite 050, which contains 4.0:2.3 Mg-Al, was attributed to the formation of the  $Al_4MgLi$

ternary phase at grain boundaries that inhibited the formation of  $\sigma(Al-Li)$ , known to be deleterious to corrosion (Ref 10-12). Alloys containing a lower concentration of  $Al_2MgLi$  and underaged showed higher resistance to corrosion than overaged alloys containing a higher proportion of grain boundary precipitates. Copper containing precipitates, such as  $Al_2CuLi$ , increased the susceptibility to pitting (Ref 8). Addition of silver in Weldalite 050 caused hardening by increasing the supersaturation of magnesium, but no adverse effect on corrosion was

observed. The advantage of Cu addition in gaining higher strength is offset by increased pitting susceptibility; hence alloy 050 offers more balanced properties in terms of strength and corrosion resistance, as shown by the investigation conducted in Arabian Gulf seawater.

The corrosion rate of Weldalite is sensitive to microstructural changes brought about mainly by variation in the Al-Li ratio. This is clearly shown by different corrosion rates of Weldalite 050 containing different Al-Li ratios. For instance, Weldalite 050 with a 4.0:2.3 Mg-Li ratio produced an increased resistance to SCC and corrosion as it was located in the Al-Li free phase field, whereas Weldalite 050 with a 5.19:2.08 (Mg-Li) ratio showed slightly lower resistance because Weldalite 050 was located in the  $\text{Al} + \text{Al}_2\text{MgLi} + \text{Al-Li}$  phase field. See Fig. 3 (Ref 13). Figure 4 shows the undesired precipitates, and Fig. 5 shows the  $\text{Al}_2\text{MgLi}$  precipitate.

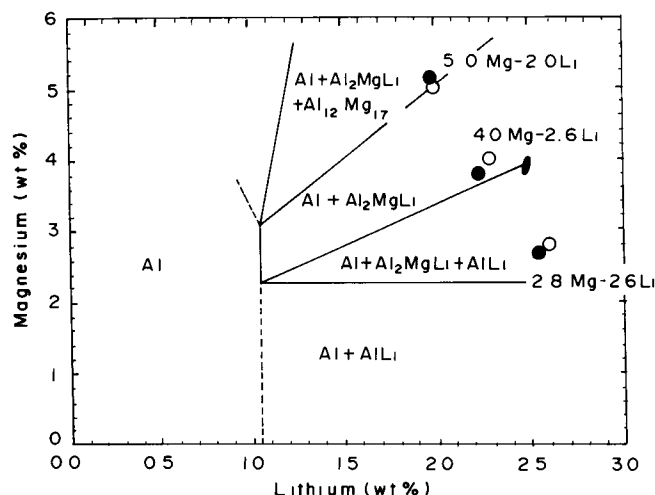


**Fig. 3** Published Al-Mg-Li phase diagram at 204 °C with the experimental alloys superimposed on it. Open circle is nominal composition, and closed circle is measured composition. From Ref 12

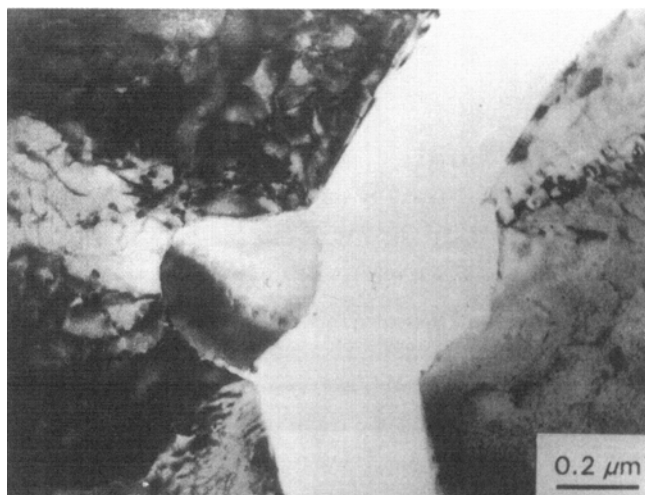


**Fig. 5** Transmission electron micrograph showing  $\text{Al}_2\text{MgLi}$  precipitates (Ref 12)

The effect of velocity on Weldalite was established in Arabian Gulf water. Table 7 shows the effect of velocity on the corrosion behavior of Weldalite 050. The resistance of the alloys to velocity is an important criteria for desalination plants and other engineering applications. The maximum corrosion rate at a velocity of 3.8 m/s is 8.923 mpy, and the minimum is 5.183 mpy at a velocity of 1.3 m/s in brackish water. The rates are relatively higher in seawater. Much lower rates are expected in a deaerated condition. In alkaline solution, where transport of hydroxide ions to the oxide solution interface controls the corrosion rate, an increase in solution velocity decreases the diffusion layer thickness, which permits a higher flux of hydroxide ions to the electrode surface and, consequently, a greater corrosion rate.

Tests conducted in modified Al-2.5 Mg alloy, (2778-0) known to be highly resistant to corrosion under static condition, exhibited a minimum corrosion rate of 9.5 mpy at a velocity of 3 m/s in North Sea water (Ref 4). All velocity tests were

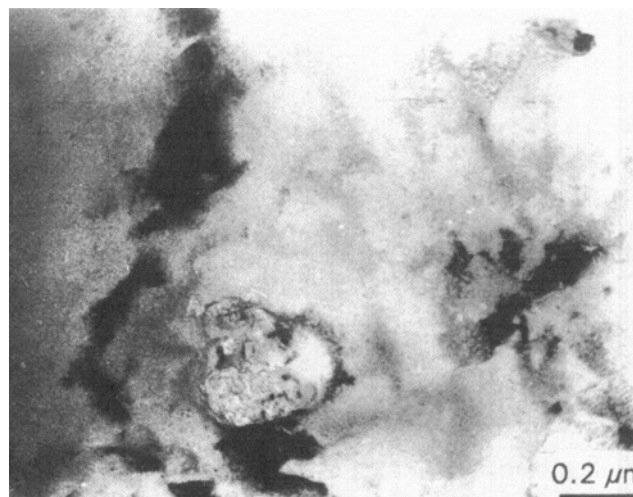


**Fig. 4** Transmission electron micrograph showing undesired precipitates (Ref 12)

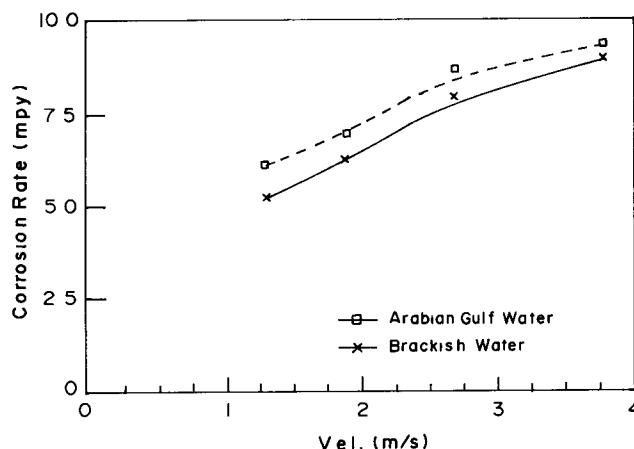


**Fig. 6** Variation in the corrosion rate of Weldalite 050 in brackish water and Arabian Gulf water

conducted in a recirculation loop made of high-density polyethylene (HDPE) (Ref 14). It consisted of an entry and exit valve, a manometer, a water pump, flow meters, and specimen holders. A manometer was used to regulate the airflow in the system. Velocity was varied by varying the diameter of the specimen holder. Tests were conducted at velocities ranging from 1 to 3.8 m/s. The corrosion rate of Weldalite 050 in aerated seawater, therefore, suggests a satisfactory resistance to corrosion at a velocity of 3.8 m/s, which is a high velocity. Figure 6 compares the corrosion rate shown in brackish water (2000 ppm TDS) with that in Arabian Gulf water at different velocities. The effect of velocity on surface morphology is shown in Fig. 7, 8, and 9. Figure 7 shows a typical pit observed in Weldalite 050 at a velocity of 2.7 m/s. Pitting at the highest velocity of 3.8 m/s is shown in Fig. 8. Corrosion products found on the surface of Weldalite 050 at a velocity of 1.9 m/s are shown in Fig. 9. The corrosion products were mainly chloride of sodium (Na) and magnesium (Mg) with smaller amounts of calcium (Ca) and iron (Fe).

Selected corrosion data on high-strength alloys 6061, 6061-SiC, and 6013-SiC are given in Table 8 for comparison (Ref 15). Weldalite 050 shows promising application poten-

tial as a high-strength material in marine environment, and its application potential in marine environment deserves further exploring.

## 4. Conclusions

Weldalite 050 belongs to the family of high-strength Al-Mg-Li alloys and shows good resistance to corrosion in Arabian Gulf water under both static and dynamic conditions. It has the capability to withstand seawater velocity up to 3.9 m/s without appreciable loss of corrosion resistance. The corrosion resistance of Weldalite 050 compares favorably with the corrosion resistance of other high-strength aluminum alloys, such as 5052, 5054, 6061, and 6013 in the wrought form and reinforced with SiC. It shows promising application potential in marine environment.

## Acknowledgments

The authors thank Martin Marietta Corporation for providing samples and some technical information. The authors also

**Table 8 Corrosion data of alloy 6013-20 SiC(P) in Arabian Gulf water**

Temperature	T4 temper			O temper			F as fabricated		
	$E_{corr}$ , mV vs SCE	$I_{corr}$ , $\mu\text{A}/\text{cm}^2$	Corrosion rate, mpy	$E_{corr}$ , mV vs SCE	$I_{corr}$ , $\mu\text{A}/\text{cm}^2$	Corrosion rate, mpy	$E_{corr}$ , mV vs SCE	$I_{corr}$ , $\mu\text{A}/\text{cm}^2$	Corrosion rate, mpy
25 °C	687	14.71	6.39	-753	18.06	7.82	-691	22.78	9.87
70 °C	760	2.72	1.18	-803	7.1	3.07	-779	7.12	3.08
100 °C	994	25.7	11.14	-1120	24.3	9.48	1016	27.71	11.91
150 °C	964	31.33	13.6	-941	47	20.37	-893	46.52	18.09
<b>Alloy 6061 (base)</b>									
300 K	...	17.75	7.65	...	...	...	...	...	...
<b>Composite [6061-Al-15 wt% SiC(P)] (extruded)</b>									
300 K	...	10.30	4.43	...	...	...	...	...	...

T4 is solutionize treated at 525 °C for 30 min, water quenched, and age hardened at room temperature. O is annealed at 350 °C for 3 h and furnace cooled. F is as fabricated. SCE is standard calomel electrode (saturated).

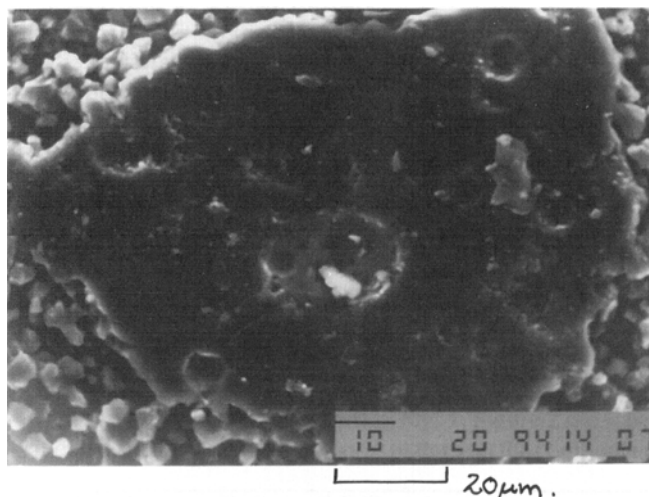


**Fig. 7** Representative micrograph of a typical pit in Weldalite 050 at a velocity of 2.7 m/s (1000×)

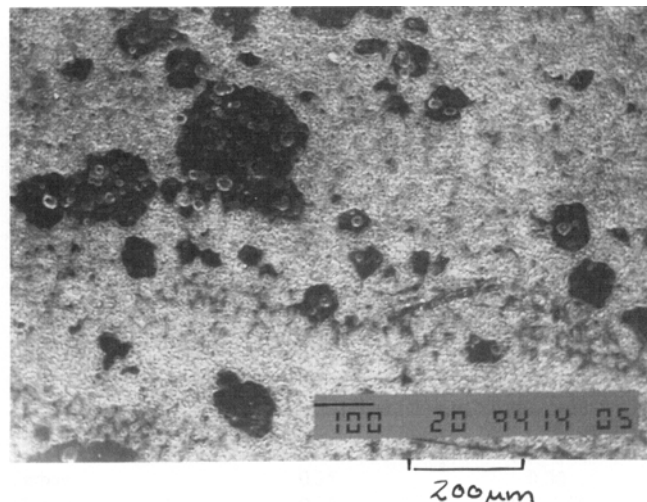


**Fig. 8** Scanning electron micrograph of pits in Weldalite 050 at a velocity of 3.8 m/s (100×)

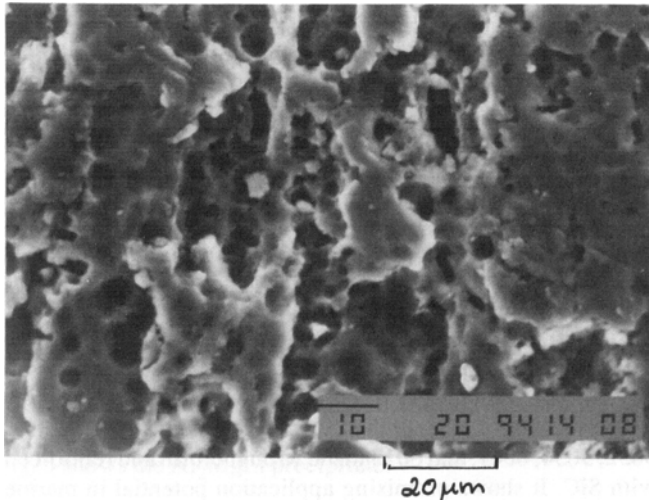


**Fig. 9** Scanning electron micrograph of corrosion products on the surface of Weldalite 050 at a velocity of 1.9 m/s (1000×)

appreciate the help given by Tim Langen. The encouragement by KFUPM is highly appreciated.

## References

1. E.D. Vernik, Jr., Dynamic Materials Testing, Aluminum Alloys for Desalination Service, *Mater. Prot.*, Vol 8 (No. 11), 1967, p 13-15
2. Y. Watnabe, Koji Nagada, and T. Nakamaru, *Corrosion Eng.*, Vol 25 (No. 5), 1976, p 323
3. C.F. Schrieber, A.L. Whitted, and F.H. Coley, "Behavior of Metals in Desalination Environment," Fourth Progress Report, Paper 62, NACE Annual Conference, National Association of Corrosion Engineers, 1971
4. G. Venkateswaran and E. Gallow, "Behavior of Some Modified Alloys in Dynamic and Nearly Static Air Saturated North Sea Water Systems," G.K.S.S., Forschungszentrum, Report G.K.S.S. 82/E, 1980
5. "Laboratory Immersion Corrosion Testing," Recommended Practical G-64, *Annual Book of ASTM Standards*, ASTM, 1992
6. Recommended Practical G-31-72, *Annual Book of ASTM Standards*, ASTM, 1994
7. E.G. Bohlmann and F.A. Posey, OSW, Proceedings 1st International Symposium on Water Desalination, (Washington, D.C., Oct. 1, 1965), p 306-325
8. R.C. Dorward and K.R. Hasse, *Corrosion*, Vol 44 (No. 12), 1988, p 932
9. T.J. Langan and J.R. Pickens, Proceedings of the 5th International Conference on Al-Li Alloys, T.H. Sanders and E.A. Starke, Ed., MCE, Birmingham, U.K., 1989, p 691
10. G.E. Thompson and B. Noble, *J. Inst. Met.*, Vol 101, 1973, p 111
11. S.F. Baumann and D.B. Williams, Proceedings of the 2nd International Conference on Al-Li Alloys, T.H. Sanders and E.A. Starke, Ed., American Society of Mechanical Engineers, 1983, p 17
12. I.J. Polmer and K.R. Sargent, *Nature*, Vol 200, 1963, p 669
13. L.S. Kramer, T.J. Langan, and J.R. Pickens, Development of Al-Mg-Li Alloys for Marine Applications, *J. Mater. Sci.*, Vol 29, 1994, p 5826
14. Z. Ahmed, Effect of Velocity on the Corrosion Behavior of Al-3Mg in North Sea Water, *Metaux*, France, Vol LVII (No. 67), 1982, p 11
15. Z. Ahmed and Abdul Aleem, B.J., KACST-AR-14-65, King Abdul Aziz City of Science and Technology, Riyadh, Dec 1994